Determination of potentially homogeneous-nucleation-based crystallization in *o*-terphenyl and an interpretation of the nucleation-enhancement mechanism

Takaaki Hikima, Yôko Adachi, Minoru Hanaya, and Masaharu Oguni*
Department of Chemistry, Faculty of Science, Tokyo Institute of Technology, Ookayama-2, Meguro-ku, Tokyo 152, Japan
(Received 26 August 1994; revised manuscript received 5 December 1994)

A homogeneous-nucleation-based crystallization was found in *o*-terphenyl in the glass-transition temperature region with an adiabatic calorimeter, and the crystallization process was investigated by direct microscopic observation. The crystallization showed its maximum rate at 248 and ceased at 250 K, while the ordinary crystal-growth process was observed to proceed only above 255 K. The two crystals formed at 248 and 297 K showed the same x-ray-diffraction patterns, indicating that they were in the same crystalline phase. The nucleation-based crystallization was observed in the temperature range of 225 to 250 K as advance of the crystal front into the liquid phase under the microscope, and the crystalline phase exhibited the appearance of the aggregation of fine crystallites which was consistent with the presence of residual entropy and the premelting property. From these results, the crystallization process was interpreted to proceed through the coalescence of crystal embryos into the crystalline phase on the liquid-crystal interface. It was concluded that the decrease in the effective interfacial energy of the embryo due to the coalescence produced an enhancement of the crystal nucleation, and that the enhancement mechanism must have played an essential role for the macroscopically observable crystallization below 250 K.

I. INTRODUCTION

Crystallization is a typical phase transition of the first order: There exists a discontinuity in the molecular arrangement and therefore in the thermodynamic quantity between liquid and crystal. The transition proceeds with two processes of nucleation and growth of crystal.[1,2] In the first process, molecules form their structural arrangement, a so-called cluster, close to that in crystal as a structural fluctuation in liquid. The cluster generally develops with decreasing temperature, implying that the homogeneous nucleation process is enhanced at low temperatures. The process is, however, suppressed at too low temperatures below the glass-transition point at which the rearrangement of molecules is frozen kinetically. In the second process, the crystal grows generally in a molecule-by-molecule fashion on the crystal surface. The growth rate is affected by the Gibbs energy difference between crystal and liquid resulting in the increase in the rate with decreasing temperature below its fusing point, but it is suppressed as the diffusion coefficient decreases at yet lower temperatures. Thus temperature dependences of homogeneous nucleation and growth rates are expected generally as illustrated in Fig. 1. The temperature regions of maximum rates for the two processes have been recognized generally as being separate.[1,2]

Classical theory of the nucleation process was proposed by Volmer and Weber[3] more than half a century ago and was extended to the crystal nucleation in liquid by Turnbull and Fisher:[4] The Gibbs energy of the crystal embryo or nucleus is expressed in terms of the sum of the interfacial energy and the Gibbs energy difference between liquid and crystal, and is expected to show a maximum at some critical radius r^* of crystal embryo/nucleus. However, to our knowledge, no direct observation of the nucleation process has been reported so far, nor has a system been known for which both the crystal nucleation rates and the Gibbs energy difference have been measured precisely as functions of temperature. Information about the nucleation rate has been obtained from experiments in which the homogeneous nucleation processes are allowed to proceed for some specified period and then the nuclei formed are counted as the number of crystal particles after being allowed to grow at some higher temperature,[5] or in which the macroscopic crystallization temperatures are measured as a function of the heating and/or cooling rate by differential thermal analysis or differential scanning calorimetry (DSC).[6] The complicated thermal history of the sample in the experiments inevitably brings some difficulties in detailed evaluation of the nucleation rates. Precise calorimetry is also lacking for evaluation of the Gibbs energies. Thus the classical theory should be investigated

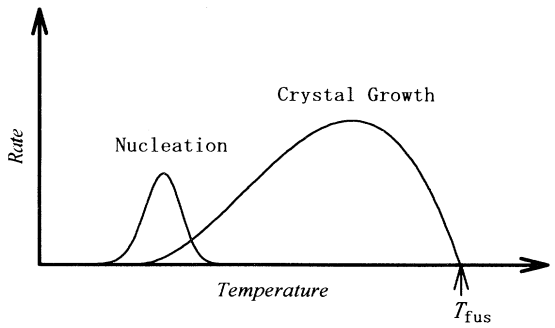

FIG. 1. A schematic diagram illustrating the variation of the rate of crystal growth and the rate of nucleation below fusing point T_{fus}.

quantitatively based on more reliable data of the nucleation rates and the Gibbs energy difference.

Molecular liquids are classified according to the "strong-fragile" concept by Angell;[7] strong liquids show temperature dependences of relaxation times of an Arrhenius type, while fragile ones those of a non-Arrhenius type. The non-Arrhenius property is reasonably interpreted to originate from the accelerated development of structured clusters with decreasing temperature.[8–10] It follows therefore that more fragile liquids would have a greater chance of homogeneous crystal nucleation on account of the emergence of more developed structured-clusters-like crystalline particles. *o*-terphenyl is known as one of the typically glass-forming and most fragile substances, and is expected to have developed clusters and a high possibility for direct observation of the crystal nucleation immediately above the glass-transition temperature region. In this respect, it is worthwhile to investigate in detail the crystallization process of *o*-terphenyl at very low temperatures. The rates of crystal growth have so far been measured by some groups[11] in the range 255–329 K, and the temperature dependence with only one peak in the rate has been observed, indicating that all the groups have observed only the process of the ordinary crystal growth in a molecule-by-molecule fashion.

In the present work, first the crystallization process of *o*-terphenyl is examined through observation of spontaneous heat evolution due to crystallization just above the glass-transition region by an adiabatic calorimetry, second, the structures of the crystals formed at different temperatures are examined by a powder x-ray-diffraction method, and thirdly the crystallization processes are observed directly with an optical microscope as a function of temperature. The potentially homogeneous-nucleation-based crystallization is indeed found immediately above the glass-transition point separately from the ordinary crystallization observed so far at high temperatures. The mechanism of the nucleation-based crystallization is discussed on the basis of the classical nucleation theory.

II. EXPERIMENT

o-terphenyl, purchased from Tokyo Chemical Ind. Co., was purified by recrystallization from the methanol solution three times and then by sublimation under reduced pressure at 320 K. Calorimetry of the purified sample was carried out with a high-precision adiabatic calorimeter previously reported.[12] The imprecision and the inaccuracy of the heat capacity were estimated to be less than ± 0.06 and $\pm 0.3\,\%$, respectively, and the imprecision of thermometry within 10^{-5} K.[12] The amount of the sample used was 16.877 g (corresponding to 0.073 279 mol) and the purity was determined by a fractional melting experiment described below to be 0.9997 ± 0.0001 in the mole fraction.

The calorimeter cell loaded with the sample was placed under adiabatic conditions by keeping the adiabatic shield, surrounding the cell, always at the same temperature as the cell and by evacuating the space within the cryostat to 10^{-4} Pa. Heat-capacity measurements were carried out by an intermittent heating method:[13] The former equilibrium temperature T_f of the cell was followed for 10 min, some specified quantity of electrical energy ΔE corresponding to the temperature increase of ~ 1.5 K was supplied into the cell in 15 min, and then the latter equilibrium temperature T_1 was followed again for 10 min. The T_1 served as T_f in the next set of heat-capacity measurements. Without any anomaly due to sample, essentially no temperature drift appeared in the temperature-rating periods under the adiabatic conditions, and the gross heat capacity of the cell was given to be ΔE divided by $\Delta T(=T_1-T_f)$. The spontaneous heat evolution or absorption associated with the enthalpy change of sample due to a glass transition and to a crystallization was monitored through observation of the spontaneous temperature drift under the adiabatic conditions of the calorimeter cell in the temperature-rating periods, since the minus rate of the enthalpy change, $-d\Delta H/dt$, was equal to the temperature drift rate, dT/dt, multiplied by the gross heat capacity of the cell under the conditions.

The powder x-ray diffractometry for the crystals formed at different temperatures was performed under ambient condition by using a Mac Science MXP[18] powder x-ray diffractometer with a Cu $K\alpha$ line.

The direct observation of the crystallization process was carried out for the purified sample in the temperature range of 224 to 260 K by using an Olympus SZ1145 microscope with a filar eyepiece and a homemade variable-temperature cold stage. The stage is shown schematically in Fig. 2.[14] The sample was melted at about 330 K between the stage and a glass cover slip under vacuum, was

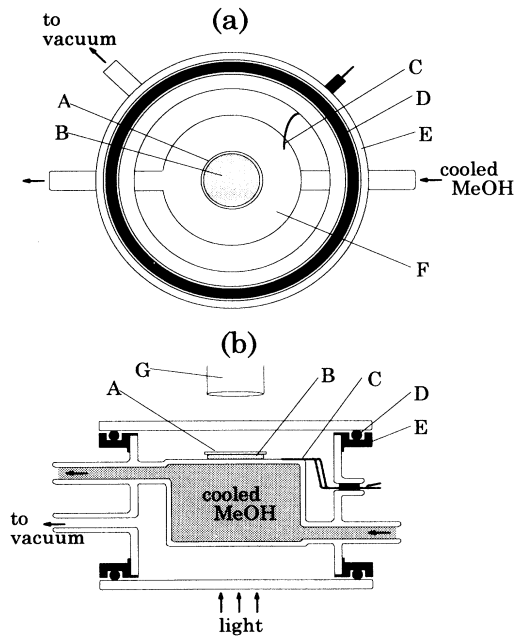

FIG. 2. Schematic sectional drawing of a variable-temperature cold stage viewed from the top (a) and from the side (b): (A) cover glass; (B) sample; (C) thermocouple; (D) o-ring gasket; (E) stainless-steel flange; (F) sample stage; (G) object lens.

quenched to the glass-transition temperature region, and then was kept at a desired temperature controlled within ±0.1 K. The thickness of the sample was confirmed not to affect the crystallization properties within its used range in the present experiment.

III. RESULTS

A. Calorimetry and x-ray diffractometry

Glass was formed within the cryostat by cooling liquid rapidly at about 8 K min^{-1} from 340 to below 180 K without crystallization. Heat capacities were measured by the intermittent heating method under the adiabatic conditions, as described above, in the temperature range between 5 and 340 K. The results of the glass are plotted in Fig. 3 with open squares together with those of two differently prepared crystals as described later. Anomalous spontaneous temperature drifts were observed in the temperature-rating periods of each series of the measurements in the direction of increasing the temperature of the glass. The drift rates of the cell are plotted with filled circles in Fig. 4. Spontaneous heat evolution first began to appear at around 190 K, showed its maximum rate at around 235 K, and then turned over to an endothermic effect having its peak at 243 K. Such a systematic temperature dependence of the spontaneous drift rates and the associated appearance of a heat-capacity jump at around 240 K are characteristic of a glass transition.[15] Further increase in the temperature gave rise to a small heat evolution effect having its peak at around 248 K and ceasing at 250 K, and to a large effect above 255 K. The heat evolution effect around 248 K became more remarkable as the sample was annealed at 248 K for longer time in advance, but it was observed to cease at 250 K in any case. The annealing at 248 K enhanced the heat evolution effect above 255 K as well; the degree of the enhancement was shown in Fig. 4 by the difference in the drift rates above 250 K between the samples subjected and not subjected to the annealing. This clearly indicates that the process proceeding at 248 K produces the enlargement of the crystal surface area and thus the heat evolution around 248 K is due to a kind of crystallization.

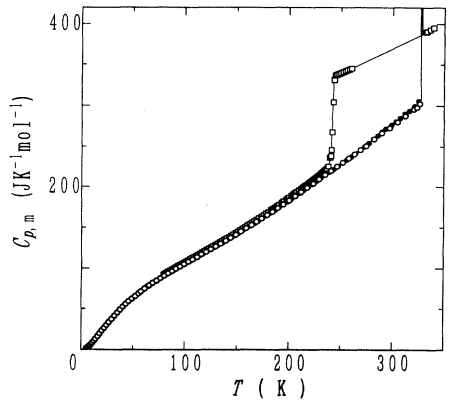

FIG. 3. Molar heat capacities of *o*-terphenyl: □ glass and liquid; ● crystal formed at 248 K; ○ crystal formed at 310 K.

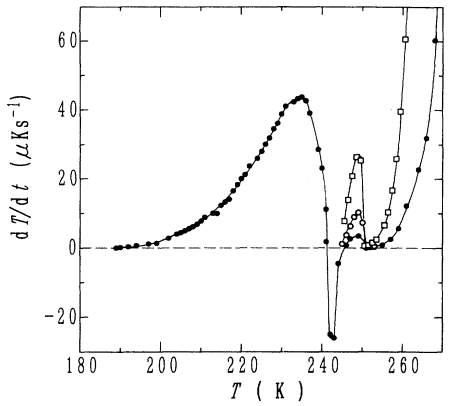

FIG. 4. Spontaneous temperature drift rates of the calorimeter cell observed under adiabatic conditions in the temperature-rating periods in the intermittent heating process for *o*-terphenyl: ● as quenched from the melt; ○ annealed at 248 K for 5 h; □ annealed at 248 K for 10 h.

When was tracked for a long time at 248 K, the heat evolution ceased in a week indicating the completion of the process. The following temperature increase up to room temperature brought no remarkable heat evolution effect and solid polycrystalline sample was found in the cell. Figures 5(a) and 5(b) show room-temperature x-ray-diffraction patterns of the polycrystals formed at 297 and 248 K, respectively. Apart from their small differences in the heights and widths, all the peaks are located at exactly the same positions between the two. This means that the processes proceeding at the two different temperatures are the crystallizations yielding the same crystalline phase. It is concluded from these structural data as well as from the ceasing of spontaneous heat evolution at 250 K that, while the effect of heat evolution above 255 K is

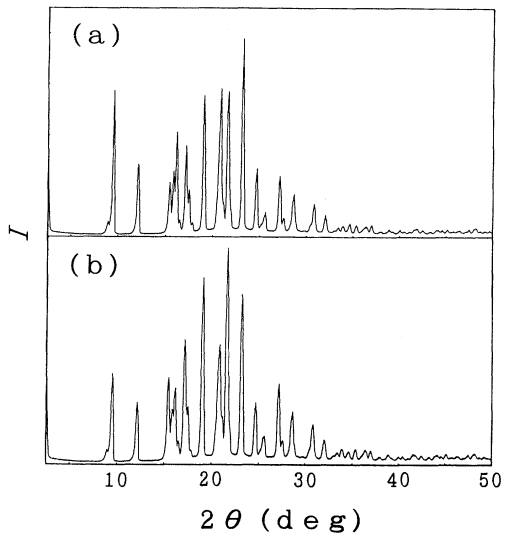

FIG. 5. Powder x-ray-diffraction patterns of the crystals formed at different temperatures: (a) crystal formed at 297 K; (b) crystal formed at 248 K.

ascribed to crystallization of the ordinary growth process, the effect around 248 K originates potentially from the crystallization based on the homogeneous nucleation due to the development of structured clusters. This conclusion is supported by the following calorimetric results of the premelting property and the presence of residual entropy of the crystal formed at 248 K; the crystal formed based on the homogeneous nucleation must be an aggregate of fine crystal nuclei.

Heat capacities of the two crystals formed at 248 and 310 K are plotted in Fig. 3 with filled and open circles, respectively. The two sets of data showed differences only in a temperature range near the fusing point. Thus a single set of fractional-melting experiments was carried out for each of the two crystals in order to examine the detailed behaviors of the fusion. The equilibration of the temperature of the calorimeter cell became sluggish during the fusion. The temperature was followed for 1 h after each intermittent energy supply, and the equilibrium temperature was estimated by extrapolating the temperature vs time curve to infinite time in terms of an exponential function. The estimated temperatures are plotted in Fig. 6 as a function of the reciprocal of fraction melted, f^{-1}. The equilibrium temperatures for the crystal formed at 310 K showed a little deviation from a linear relation, as were fitted well by the Mastrangelo's equation shown by a solid line.[16] From the fitting, the fusing temperature was given to be (329.38±0.01) K and the mole-fraction purity to be (0.9997±0.0001), respectively. The apparent equilibrium temperatures for the crystal formed at 248 K indicated that the fusion began at an appreciably lower temperature than that of the crystal formed at 310 K. The extrapolation of the temperatures toward $f^{-1}=0$ in terms of the Mastrangelo's equation yielded the fusing temperature of (329.37±0.01) K which was lower by 0.01 K than that of the crystal formed at 310 K. These can be only reasonably understood if the crystal formed at 248 K is composed of fine crystallites. The crystallite has a larger Gibbs energy on account of its smallness in size compared to the bulk crystal so that it should melt at a relatively lower temperature.

Figure 7 shows the molar entropies of glass, liquid, and two batches of crystals as functions of temperature, on the assumption that the zero-point entropy of the crystal formed at 310 K is zero. The entropies were evaluated according to the following standard equation; $S(T)=S(0)+\int_0^T (C_{p,m}/T)dT$, where $S(0)$ denotes some residual entropy remaining even at 0 K, and the entropies of all the samples were equated to be equal to one another in the liquid state above the fusing point. Here the heat capacities below 5 K were approximated by the Debye low-temperature equation, $C_{p,m}(T)=aT^3$; a was determined by using the experimental data between 5 and 7 K to be 0.0103 $\mathrm{J\,K^{-4}\,mol^{-1}}$ and 0.00919 $\mathrm{J\,K^{-4}\,mol^{-1}}$ for the crystals formed at 248 and 310 K, respectively. The inset shows the temperature dependences approaching 0 K on an enlarged scale. The residual entropy of the crystal formed at 248 K was found, taking the imprecision of the heat-capacity data into consideration, to be (0.5±0.3) $\mathrm{J\,K^{-1}\,mol^{-1}}$ which was quite small but appreciable. The presence of the finite residual entropy is consistent with the interpretation that the sample is the aggregate of crystal nuclei; namely, the configurational degrees of freedom of a considerable number of molecules present around the interface between the crystal particles as well as those of the particles themselves would give rise to some disorder within the aggregate.

B. Microscopic observation

The crystallization below 250 K was observed to begin with an accidental emergence of crystallite, and it proceeded as an enlargement of the crystalline phase with the advance of the crystal front into the liquid phase as the ordinary crystal-growth process above 255 K proceeded. The liquid-crystal interface was revealed to be

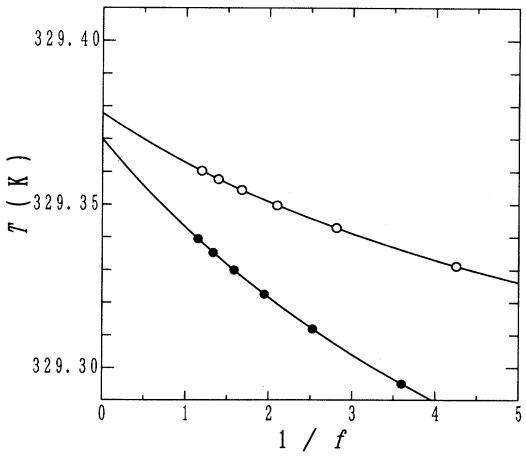

FIG. 6. Equilibrium temperatures of fusion vs the reciprocal of fraction melted for the crystals formed at two different temperatures: ○ crystal formed at 310 K; ● crystal formed at 248 K. Solid lines represent the results of the fitting in terms of the Mastrangelo's equation.

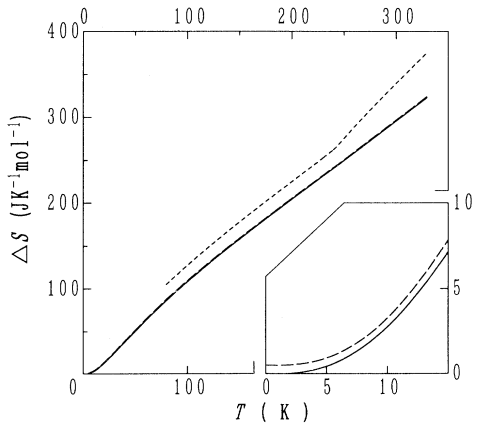

FIG. 7. Molar entropies of *o*-terphenyl estimated from the heat-capacity data: · · · ·, glass and liquid; — — —, crystal formed at 248 K; ——, crystal formed at 310 K. Inset shows the temperature dependences approaching 0 K on an enlarged scale.

smooth through the microscope with a resolving power of 1 μm order, but the crystalline sample appeared to be the aggregate of fine crystallites while that formed above 255 K appeared to be the gathering of relatively large crystals with the respective particular orientations. The observed manner of crystallization explains clearly the enhancement of the heat-evolution effect by the annealing treatment at 248 K in the calorimetry, since the enlargement of the crystal front area within the cell increases the places where the crystallization potentially takes place.

Since the crystallization process below 250 K was observed as the advance of the crystal front into the liquid phase, the growth rate of the crystalline phase was evaluated from the advancement length of the front in a specified period. The rates obtained in the temperature range between 220 and 260 K are plotted in Fig. 8 together with those at higher temperatures reported in the literature.[17] The growth rate increased continuously with increasing temperature from 220 to 248 K, showing its peak of about 0.018 μm s^{-1} at around 248 K, but the growth ceased suddenly at 250 K as it ceased in the calorimetry. Further increase in the temperature brought the ordinary crystal growth to occur, and the growth rates obtained above 255 K were in good agreement with previously reported values.[17]

Figure 9 shows the difference between the progress of crystallization after a temperature jump from 247 to 263 K and the reverse from 263 to 247 K. In the former case, the crystal front advanced immediately after the jump, keeping the front line smooth and at the rate expected at 263 K. In the latter case, on the other hand, no continuous advance was observed of the crystal front which was formed at 263 K. The crystallization instead began with forming nuclei heterogeneously at some spots on the liquid-crystal interface and proceeded with forming a circular crystal front about each nucleus at the advance rate expected at 247 K. These observations clearly indicate that the crystal-growth processes are different between above 255 and below 250 K. The observation that the growth rate above 255 K is rather independent of the crystal surface, is consistent with the interpretation that the crystallization proceeds in the molecule-by-molecule manner. The growth process below 250 K is deduced to be considerably affected by the microscopic structure of the crystal surface. This is also consistent with the interpretation that the crystallization below 250 K is brought through union of the structured cluster of crystal embryo or nucleus on the crystal surface.

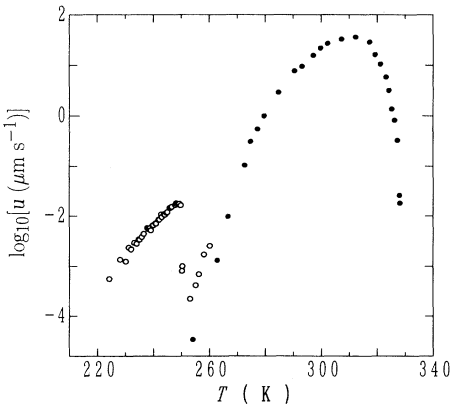

FIG. 8. Crystal-growth rate vs temperature relation for *o*-terphenyl: ○ data obtained in this work; ● data from Ref. 13.

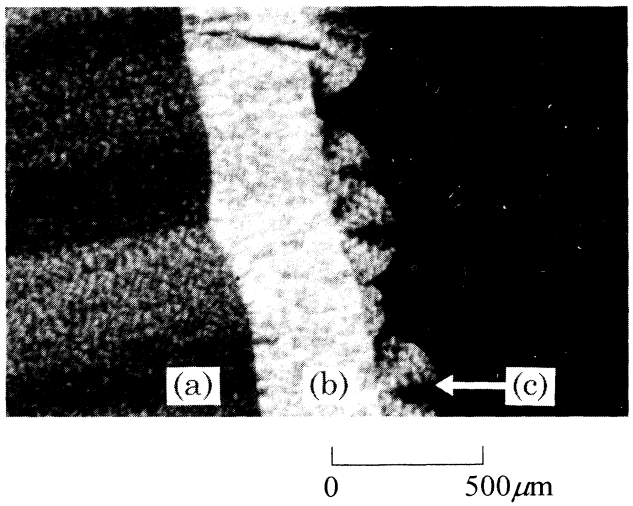

FIG. 9. Photomicrograph of crystalline *o*-terphenyl growing into the supercooled liquid: (a) crystalline layer formed at 247 K; (b) crystalline layer formed at 263 K after a temperature jump from 247 K; (c) fan-shaped crystal formed at 247 K after a temperature jump from 263 K.

Figure 10 illustrates the temperature regions in which the glass transition, the potentially homogeneous-nucleation-based crystallization, and the ordinary crystallization phenomena were found by calorimetry (a) and by optical-microscopic observation (b). The region of glass

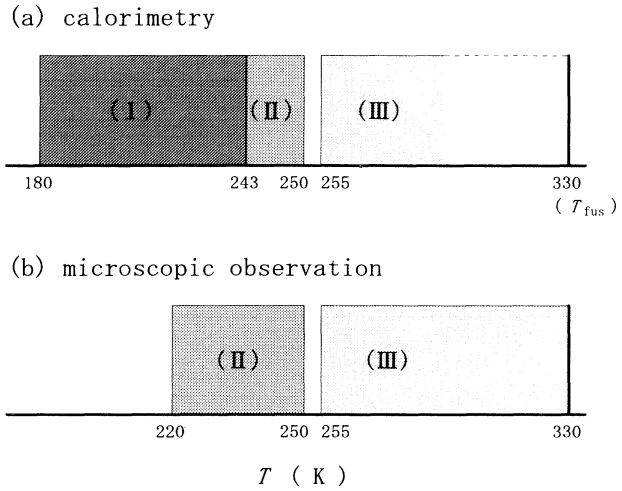

FIG. 10. Diagram showing the temperature regions of the glass transition (I), the potentially homogeneous-nucleation-based crystallization (II), and the ordinary crystallization (III): (a) found by the calorimetry; (b) found by the microscopic observation.

transition is lacking in the diagram (b) in that the microscopic observation is inadequate for investigation of the glass transition. Thus the nucleation-based crystallization could be detected by the method without interference of the glass-transition phenomenon. It is noted that the nucleation-based crystallization was observed with increasing temperature by both methods to cease suddenly at 250 K and to be completely separate in the temperature region from the ordinary crystal-growth process found above 255 K. Any theory which has been proposed so far for crystal growth cannot explain such an anomalous temperature dependence especially of the growth rates shown in Fig. 8.

IV. DISCUSSION

A. Mechanism of homogeneous-nucleation rate enhancement in the crystal growth

The classical theory of homogeneous crystal nucleation is given as follows. Assuming the spherical form for crystal embryo and nucleus, size dependence of the Gibbs energy of the embryo ΔG can be expressed as

$$\Delta G = -\frac{4}{3}\pi r^3 \Delta G_V + 4\pi r^2 \sigma \ , \tag{1}$$

where r is radius of the embryo, ΔG_V is the difference in the Gibbs energy between crystal and liquid phases per unit volume, and σ is the interfacial energy per unit area of the embryo facing the liquid.[1,2] In view of the powers of r in the two terms on the right-hand side of Eq. (1), the ΔG has the maximum value ΔG^* at some critical radius r^* at any temperature below a fusing point, as is represented by any solid line in Fig. 12. Once the embryo has a size larger than r^*, it tends to grow to a crystal nucleus having a lower Gibbs energy than ΔG^*. The embryo of the critical radius is called a critical nucleus, and following expressions for r^* and ΔG^* can be deduced from Eq. (1) according to the critical condition of $d\Delta G/dr = 0$ at $r = r^*$;[1,2]

$$r^* = \frac{2\sigma}{\Delta G_V} \tag{2}$$

and

$$\Delta G^* = \frac{16\pi\sigma^3}{3\Delta G_V{}^2} . \tag{3}$$

The Gibbs energy difference between liquid and crystal in o-terphenyl can be derived from the present heat-capacity data, as is shown in Fig. 11. Meanwhile, in the present work, the interfacial energy of $\sigma = 12.6$ mJ m^{-2} was used as it had been reported by Onorato, Uhlmann, and Hopper on the basis of their DSC experiment.[6] Figure 12 shows the ΔG vs r relations evaluated at three different temperatures of 220, 250, and 280 K. Increasing temperature brings the enlargement of both the size r^* and the Gibbs energy ΔG^* of critical nucleus. Uhlmann *et al.* expressed the steady-state homogeneous nucleation rate I_V per unit volume in liquid as

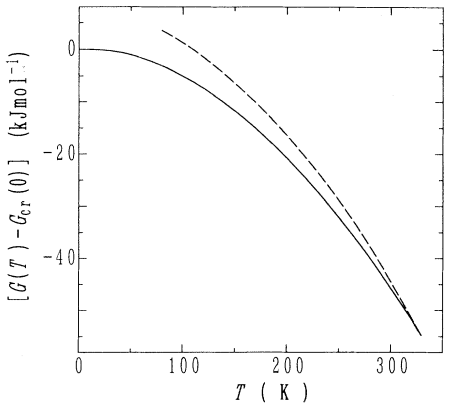

FIG. 11. Gibbs energy diagram for o-terphenyl derived from the heat-capacity data: — — —, glass and liquid; ——, crystal formed at 310 K.

$$I_V \approx N_V \nu \exp\left[-\frac{\Delta G^*}{kT}\right] . \tag{4}$$

Here N_V is the number of molecules per unit volume since any molecule has a chance to become the central one for formation of the critical nucleus, ν is the frequency of molecular transport across the interface between embryo/nucleus and liquid, and k is Boltzmann's constant.[18,19] The ν has been ordinarily related to the bulk viscosity η through the Stokes-Einstein relation[18]

$$\nu \approx kT/3\pi a_0^3 \eta \ , \tag{5}$$

where a_0 is molecular diameter. Then Eq. (4) is transformed to

$$I_V \approx \frac{N_V kT}{3\pi a_0^3 \eta} \exp\left[-\frac{16\pi\sigma^3}{3\Delta G_V^2 kT}\right] . \tag{6}$$

I_V is generally quite small at high temperatures on account of the small values of ΔG_V, and increases with increase in the ΔG_V as the temperature is lowered. It is

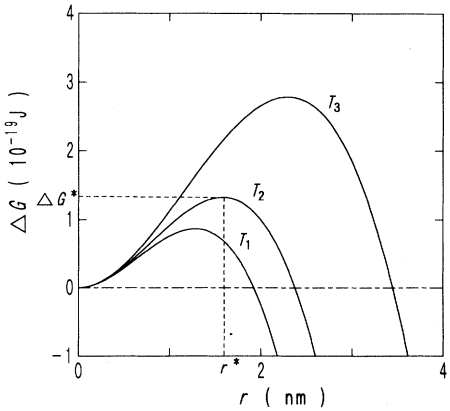

FIG. 12. Gibbs energy of a spherical crystal embryo/nucleus as a function of the radius at three different temperatures: $T_1 = 220$ K, $T_2 = 250$ K, and $T_3 = 280$ K.

also quite small at very low temperatures on account of the large values of η, and increases with decrease in the η as the temperature is raised. Thus the nucleation rate I_V has a maximum at some temperature as it is depicted in the case of *o*-terphenyl with a curve (d) in Fig. 13.

The homogeneous-nucleation-based crystallization process was observed to proceed as the advance of the crystal front into the liquid phase under the microscope, and no crystal particle was observed to emerge in the central part of liquid sample. These indicate that a certain mechanism of homogeneous-nucleation rate enhancement must operate on the liquid-crystal interface. The homogeneous nucleation rate, as is indicated by Eq. (4), is mainly dominated by the magnitude of ΔG^* and thus by the interfacial energy σ through Eq. (3). When the nucleation proceeds within the range of r^* from the liquid-crystal interface, the embryo formed will make contact with the crystal, and the contact is expected to decrease the effective interfacial energy on account of the decrease in its area being in contact with liquid. This situation is schematically illustrated in Fig. 14, in which cases (a), (b), (c), and (d) show the nucleation at the point in the liquid phase apart from the interface by 0, $0.2r^*$, $0.5r^*$, and r^*, respectively. In cases (a), (b), and (c), embryos with sizes smaller than r^* can make contact with the crystalline phase resulting in reduction of the effective interfacial energies of embryos, and this effect produces the large change in ΔG^*. Lines (a), (b), and (c) in Fig. 15 represent the Gibbs energies of the embryos ΔG as functions of radius r in cases (a), (b), and (c), respectively, in Fig. 14. The critical values of the Gibbs energies, ΔG^*(a), ΔG^*(b), and ΔG^*(c), are considerably reduced compared with ΔG^* in case (d) where no reduction of the interfacial energy occurs, while the critical radii r^*(a), r^*(b), and r^*(c) do not differ very much from r^* in case (d). The calculated critical Gibbs energies ΔG^* are tabulated in Table I together with the nucleation rates evaluated from the ΔG^* values according to Eqs. (4) and (5). The maximum nucleation rates of the I_V(a), I_V(b), and I_V(c), which are shown in Fig. 13, amount to 3×10^9, 1×10^9, and 7×10^6 times, respectively, the rate of the original homogeneous crystal nucleation, I_V(d). This demonstrates that the nucleation rate is enhanced drastically by the decrease in the interfacial energy. This decrease is interpreted to be the very nucleation-enhancement mechanism enabling the homogeneous-nucleation-based crystallization to be observed and dominating the crystallization process at very low temperatures.

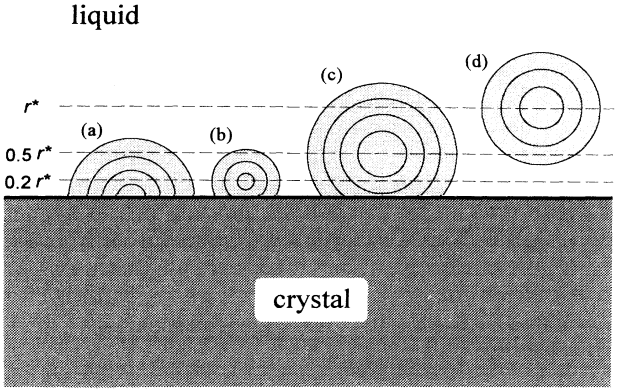

FIG. 14. Schematic diagram illustrating the formation of embryos/nuclei nearby the liquid-crystal interface: (a) formation at a point just on the liquid-crystal interface; (b) formation at a point in the liquid apart by $0.2r^*$ from the interface; (c) by $0.5r^*$; (d) by r^*.

B. Evaluation of the crystal-growth rate based on the classical theory and its comparison with the experimental result

Assuming that the crystal front advances into the liquid phase through taking the homogeneously formed critical nuclei into the crystalline phase on the liquid-

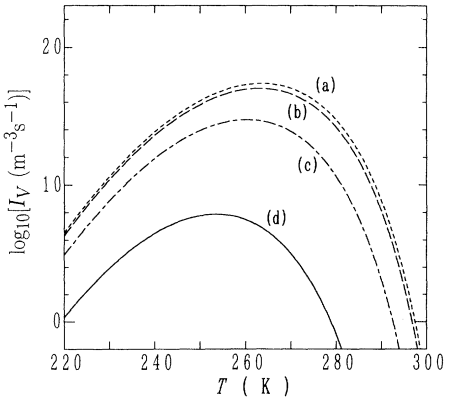

FIG. 13. Temperature dependences of the calculated homogeneous-nucleation rates of *o*-terphenyl: (a) nucleation at a point just on the liquid-crystal interface; (b) nucleation at a point apart by $0.2r^*$ from the interface; (c) by $0.5r^*$; (d) by r^*. Here viscosity data were taken from the result by Laughlin and Uhlmann (Ref. 20). See text for the detail.

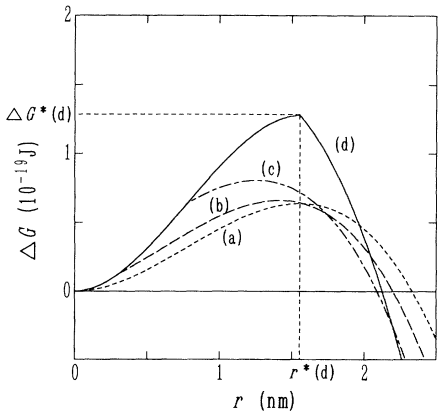

FIG. 15. Gibbs energy of a spherical crystal embryo/nucleus calculated at 248 K as a function of the radius with including the effect of the reduction in the interfacial energy on the liquid-crystal interface: (a) embryo/nucleus formed at a point just on the liquid-crystal interface; (b) embryo/nucleus formed at a point in the liquid phase apart by $0.2r^*$ from the liquid-crystal interface; (c) by $0.5r^*$; (d) by r^*.

TABLE I. Calculated values for the critical Gibbs energy of the embryo ΔG^* and the nucleation rate I_V in *o*-terphenyl at 254 K.[a]

l/r^*[b]	$\Delta G^*/\Delta G_0^*$[c]	I_V/I_{V0}[d]
0.2	0.51	10^9
0.5	0.64	10^7
>1	1	1

[a]The temperature at which the calculated homogeneous nucleation rate had maximum value [see the solid line (a) in Fig. 9].

[b]l and r^* denote the distance of the center of embryo from the liquid-crystal interface and the critical radius of the embryo, respectively.

[c]ΔG_0^* represents the critical Gibbs energy of the embryo making no contact with the crystal.

[d]I_{V0} represents the homogeneous nucleation rate calculated in the case with no interfacial energy of the embryo being quenched.

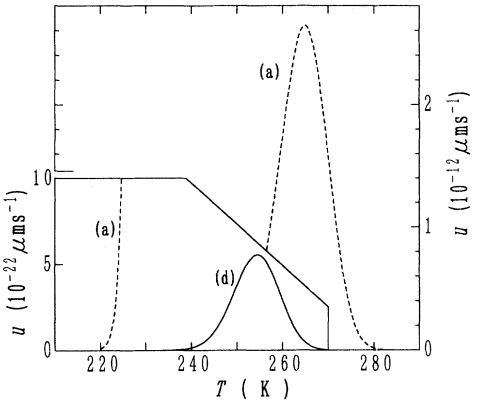

FIG. 16. Temperature dependence of the calculated growth rates due to the homogeneous-nucleation-based crystallization in *o*-terphenyl: (a) nucleation at a point just on the liquid-crystal interface; (d) nucleation at a point in the liquid phase apart by r^* from the liquid-crystal interface.

crystal interface, the advance rate u can be related to the value of I_V as follows: The crystalline surface, when covered with a layer of critical nuclei, gains its advancement by $2r^*$. The number of the nuclei to cover the surface area of A is of the order of $A/(2r^*)^2$, and the frequency of the crystal nucleation in the region apart by r^* from the surface is approximated to be $I_V Ar^*$. The time required for the crystal front to advance by $2r^*$ is then roughly estimated to be $A/[(2r^*)^2(I_V Ar^*)]$. Thus u is expressed to a rough approximation by the relation

$$u \approx 2r^* \frac{(2r^*)^2(I_V Ar^*)}{A} = 8I_V(r^*)^4 . \quad (7)$$

Temperature dependence of the growth rate can be evaluated according to Eqs. (4) and (7); curves (a) and (d) in Fig. 16 represent the rates evaluated for cases (a) and (d) in Fig. 14, respectively. The maximum rate in case (d), in which no reduction in the interfacial energy occurs, is estimated to be $\sim 10^{-22}$ μm s^{-1}. The rate is smaller by 20 orders of magnitude than the observed growth rate of $\sim 10^{-2}$ μm s^{-1}, indicating that the accumulation process of critical nuclei is definitely unobservable macroscopically. This is consistent with the fact that no crystal nucleation is observed in the central part of the liquid sample where no reduction in ΔG^* occurs in the process. The maximum rates in cases (a)–(c) with the reduction in the interfacial energy are estimated to be $\sim 10^{-12}$, $\sim 10^{-13}$, and $\sim 10^{-15}$ μm s^{-1}, respectively. The rates are strikingly enhanced as compared with that in case (d); the enhancement factors amount to 10, 9, and 7 orders of magnitude, respectively. This enhancement mechanism is thus concluded to play an indispensable role for the macroscopic crystallization at such low temperatures as the glass-transition temperature.

Concerning the absolute value of the advanced rate u, however, there still exists a large discrepancy of ten orders of magnitude between the observed maximum value 10^{-2} μm s^{-1} and the above-evaluated maximum 10^{-12} μm s^{-1}. Further, the characteristic behavior that the advance ceases rather suddenly at 250 K is yet still unexplained at present. More detailed investigation is required in the future, including improvement of the classical nucleation theory itself which has been applied to the crystallization in liquid.

V. CONCLUSION

A potentially homogeneous-nucleation-based crystallization was discovered in the present study in fragile liquid *o*-terphenyl as a phenomenon of the crystal front advancing into the liquid phase at very low temperatures. The observable crystallization was reasonably interpreted, on the basis of the classical nucleation theory, to occur due to the decrease in the interfacial energy of the crystal embryo by making contact with the crystal on the liquid-crystal interface. This means also that, in the temperature region where the homogeneous-nucleation-based process is dominant, the crystallization proceeds with the formation of a polycrystal but not a single crystal. Considering that the fragility of liquid corresponds with the accelerated development of structured clusters of molecules with decreasing temperature and that part of the clusters correspond with the crystal embryos, the homogeneous-nucleation-based crystallization would be observed in the future in many systems of fragile liquids. The accumulated and detailed observations of the processes and the theoretical explanation of the results are expected to make progress toward complete understanding of the crystal nucleation process as an important initial, as yet still unclear, step of the whole crystallization.

ACKNOWLEDGMENT

This work was supported partly by a Grant-in-Aid for Scientific Research from the Ministry of Education, Science and Culture, Japan.

*Author to whom correspondence should be directed.

[1]C. N. R. Rao and K. J. Rao, *Phase Transitions in Solids* (McGraw-Hill, New York, 1978), p. 82.
[2]A. E. Owen, in *Amorphous Solids and the Liquid State* (Plenum, New York, 1985), p. 395.
[3]M. Volmer and A. Weber, Z. Phys. Chem. **119**, 277 (1926).
[4]D. Turnbull and J. C. Fisher, J. Chem. Phys. **17**, 71 (1949).
[5]P. F. James, Phys. Chem. Glasses **15**, 95 (1974).
[6]P. I. K. Onorato, D. R. Uhlmann, and R. W. Hopper, J. Non-Cryst. Solids **41**, 189 (1980).
[7]C. A. Angell, J. Non-Cryst. Solids **131-133**, 13 (1991).
[8]G. Adam and J. H. Gibbs, J. Chem. Phys. **43**, 139 (1965).
[9]H. Fujimori, H. Fujita, and M. Oguni, Bull, Chem. Soc. Jpn. **68**, 447 (1995).
[10]H. Fujimori and M. Oguni, Solid State Commun. **94**, 157 (1995).
[11]R. J. Greet, J. Cryst. Growth **1**, 195 (1967); G. Scherer, D. R. Uhlmann, C. E. Miller, and K. A. Jackson, *ibid.* **23**, 323 (1974).
[12]H. Fujimori and M. Oguni, J. Phys. Chem. Solids **54**, 271 (1993).
[13]E. F. Westrum, Jr., G. T. Furukawa, and P. J. McCullough, *Calorimetry of Non-Reacting Systems,* in Experimental Thermodynamics, Vol. 1 (Butterworths, London, 1968), p. 133.
[14]H. Yamada, M. Hanaya, Y. Kanno, T. Kikuchi, and S. Onodera, Bull. Inst. Chem. Reac. Sci. Tohoku Univ. **2**, 39 (1992).
[15]H. Suga and S. Seki, Faraday Discuss. Chem. Soc. **69**, 221 (1980).
[16]S. V. R. Mastrangelo and R. W. Dornte, J. Am. Chem. Soc. **77**, 6200 (1955).
[17]J. H. Magill and Hin-Mo Li, J. Cryst. Growth **20**, 135 (1973).
[18]D. R. Uhlmann, *Materials Science Research, Vol. 4* (Plenum, New York, 1969), p. 172.
[19]H. Yinnon and D. R. Uhlmann, J. Non-Cryst. Solids **44**, 37 (1981).
[20]W. T. Laughlin and D. R. Uhlmann, J. Phys. Chem. **76**, 2317 (1972).

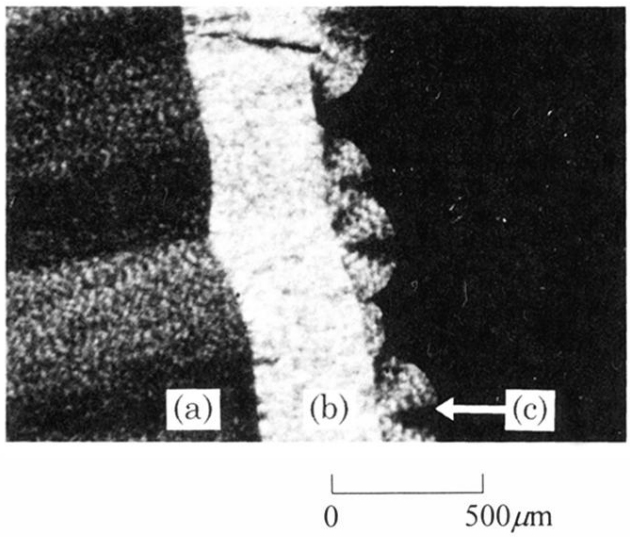

FIG. 9. Photomicrograph of crystalline *o*-terphenyl growing into the supercooled liquid: (a) crystalline layer formed at 247 K; (b) crystalline layer formed at 263 K after a temperature jump from 247 K; (c) fan-shaped crystal formed at 247 K after a temperature jump from 263 K.